Chemical Engineering Journal 225 (2013) 216–222

Contents lists available at SciVerse ScienceDirect

Chemical Engineering Journal

journal homepage: www.elsevier.com/locate/cej

Anionic stilbene intercalated layered double hydroxide with two-photon excited polarized photoemission

Dongpeng Yan, Jun Lu *, Min Wei *, David G. Evans, Xue Duan

State Key Laboratory of Chemical Resource Engineering, Beijing University of Chemical Technology, Beijing 100029, PR China

HIGHLIGHTS

- A stilbene derivate intercalated layered double hydroxides have been prepared.
- The samples exhibited changeable fluorescent properties.
- The film showed polarized photoemission with one-photon and two-photon excitation.

ARTICLE INFO

Article history:
Received 12 December 2012
Received in revised form 22 February 2013
Accepted 7 March 2013
Available online 25 March 2013

Keywords:
Hybrid materials
Layered double hydroxide
Thin film
Luminescence
Two-photon

ABSTRACT

Two-photon solid-state fluorescence materials have received much attraction due to their wide optoelectronic applications. Herein, organic–inorganic hybrid two-photon fluorescence materials have been prepared by the introduction of a sulfonated stilbene (BSB, 4,4′-bis(2-sulfonatostyryl) biphenyl) assembled into layered double hydroxide (LDH) matrix. The structure and chemical composition of the composites were characterized by X-ray diffraction, elemental analysis, thermogravimetry and differential thermal analysis (TG–DTA). Fluorescence spectra demonstrate that the fluorescent properties (such as emission wavelength and photoluminescence quantum yield (PLQY)) of the as-obtained samples can be tuned by changing the layered charge density and chemical composition, in which the BSB/Zn_3Al–LDH sample exhibited the highest emission intensity and PLQY. Moreover, the BSB/Zn_3Al–LDH film was further fabricated by a solvent evaporation method, and the film exhibited well-defined one-photon and two-photon excited polarized photoemission with the anisotropy of *ca.* 0.12. It can be expected that these BSB/LDH systems can serve as a good candidate for new type of solid-state up-conversion and polarized fluorescent materials.

1. Introduction

The organic chromophores with two-photon fluorescence have recently received much attraction for optoelectronic applications such as optical sensor [1], nonlinear optics [2], photoconductors [3], photovoltaics [4], and up-conversion emission [5]. Unlike many common one-photon fluorescent molecules (such as rhodamine and cyanine) with very small Stokes shifts [6,7], which can result in serious self-quenching and fluorescence detection errors, the two-photon fluorescent materials involving anti-Stokes shifts can overcome such disadvantage and also reduce the excitation backscattering effects effectively. These properties are beneficial for the chromophores in the field of fluorescent image [8]. However, luminescent dye molecules with conjugated structures are prone to the formation of aggregation in the solid state, resulting in red-shift of fluorescence, broadening and even quenching [9]. This is unfavorable for the construction of high-performance two-photon luminescent materials. Moreover, the relatively poor thermal or optical stability usually restrict these two-photon excited materials into optoelectronic applications. To overcome these disadvantages, great efforts have been devoted to design and synthesize new types of two-photon fluorescence molecules; unfortunately, the time-consuming synthesis process and relative low yield often limit their development [10]. Therefore, it is of importance to realize novel two-photon emissive materials with both high thermal/chemical stability and enhanced optical properties.

Recently, great interest has been paid on the assembly of two-dimensional (2D) ordered inorganic–chromophore materials by incorporating chromophore molecules into solid host matrices, since they may show alternated functionalities (such as enhanced photo-, thermal- and mechanical-stabilization) compared with their individual components alone [11]. In this regard, layered

* Corresponding authors. Tel.: +86 10 64412131; fax: +86 10 64425385 (M. Wei).
E-mail addresses: lujun@mail.buct.edu.cn (J. Lu), weimin@mail.buct.edu.cn (M. Wei).

1385-8947/$ - see front matter © 2013 Elsevier B.V. All rights reserved.
http://dx.doi.org/10.1016/j.cej.2013.03.038

double hydroxides (LDHs), whose structure can be generally expressed as the formula $\left[M^{II}_{1-x}M^{III}_{x}(OH)_2\right]^{x+}A^{n-}_{x/n}\cdot yH_2O$ (M^{II} and M^{III} are divalent and trivalent metals respectively; A^{n-} is the guest anion), are one type of anionic layered host matrices [12]. Several luminescent molecules, such as organic small anions [13], π-conjugated polymers [14] and photoactive complexes [15], have been intercalated into LDH layers to achieve luminescent materials with superior luminous efficiency due to the host–guest interactions. Furthermore, the regular arrangement of dye molecules within the LDHs can exhibit specific anisotropic photoemission behaviors, owning to the intrinsic anisotropy of the LDHs with 2D lamellar structure [16]. However, to the best of our knowledge, the incorporation of fluorescent dye anions into LDHs to obtain luminescence properties with two-photon emission has scarcely been reported.

Phenylenevinylene and stilbene-type compounds have attracted considerable interest because of their excellent optical and electronic properties [17–19]. In addition, they are at present the most commonly used organic two-photon-excited luminescence materials, and it is still highly desirable to achieve tunable and enhanced fluorescent performances for stilbene-based materials. The intercalation assembly principle inspires us to develop new types of inorganic–organic hybrid system by the introduction of stilbene derivatives into LDH layer, which would exhibit the following advantages: (1) the rigid and confined space imposed by LDH layers can inhibit the thermal vibration and rotation of stilbene anions relating to the nonradiative relaxation process of their exciting states, and also achieve an ordered and regular microenvironment for the interlayer anions [17]; (2) the presence of inorganic LDH monolayers can improve the thermal and optical stability of the interlayer anions, which can meet the need for the improvement of thermal and photostability of fluorescent molecules for long-term application [18].

In this work, a sulfonated derivate of stilbene (BSB, 4,4′-bis(2-sulfonatostyryl) biphenyl, Scheme 1) assembled into the interlayer of the LDHs with different layer charge density and chemical composition have been prepared by a co-precipitation method. The obtained BSB/LDH compositions show tunable optical properties (such as emission wavelength, photoluminescence quantum yield and two-photon photoemission), in which the sample BSB/Zn_3Al–LDH exhibits the optimal luminescent properties, higher than the pure BSB and other intercalation products. Moreover, the BSB/LDH system presents well defined two-photon-excited photoemission behavior upon excitation by near-infrared light, demonstrating that the as-prepared BSB/LDH systems can be potentially applied as new types of two-photon-excited fluorescent materials.

2. Experimental details

2.1. Reagents and materials

Disodium 4,4′-bis (2-sulfonatostyryl) biphenyl (BSB) was purchased from Sigma Chemical. Co. Ltd. Analytical grade $Mg(NO_3)_2\cdot 6H_2O$, $Zn(NO_3)_2\cdot 6H_2O$, $Co(NO_3)_2\cdot 6H_2O$, $Ni(NO_3)_2\cdot 6H_2O$, and $Al(NO_3)_3\cdot 9H_2O$ were purchased from Beijing Chemical Co. Ltd. and used without further purification.

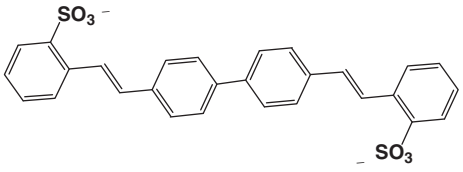

Scheme 1. Molecular structure of 4,4′-bis(2-sulfonatostyryl) biphenyl (BSB) anion.

2.2. Preparation of the BSB/LDHs

BSB/LDH composites were prepared by the coprecipitation method. The matched molar ratio of Mg^{2+} (Zn^{2+}, Co^{2+}, Ni^{2+})/Al^{3+}/BSB were 2.0 (or 3.0): 1.0: 0.5 in these experiments. Taking the BSB/Mg_2Al–LDH sample as an example, 100 ml of solution containing $Mg(NO_3)_2\cdot 6H_2O$ (0.02 mol) and $Al(NO_3)_3\cdot 9H_2O$ (0.01 mol) was slowly added dropwise to 100 ml of solution containing NaOH (0.06 mol) and BSB (0.005 mol) with vigorous agitation under a nitrogen flow. The pH value at the end of addition was adjusted to 8.0 by further addition of 2.4 mol/L NaOH solution. The reaction mixture was subsequently heated at 70 °C for 24 h, filtered, and the resultant solid washed thoroughly with deionized water and finally vacuum-dried at 50 °C for 15 h. The film of BSB/LDH was prepared by a solvent evaporation method: a suspension of the as-prepared BSB/LDH powder in 20 mL of ethanol (1 mg/mL) was ultrasonically dispersed and then spread on a quartz (3 cm × 3 cm) which was cleaned thoroughly by an ultrasonic anhydrous ethanol bath.

2.3. Characterization

The samples of BSB/LDH were characterized on a Rigaku D/MAX2500VB2+/PC X-ray diffractometer, using Cu Kα radiation (0.154184 nm) at 40 kV, 30 mA with a scanning rate of 5°/min, a step size of 0.02°/s, and a 2θ angle ranging from 3° to 70°. The

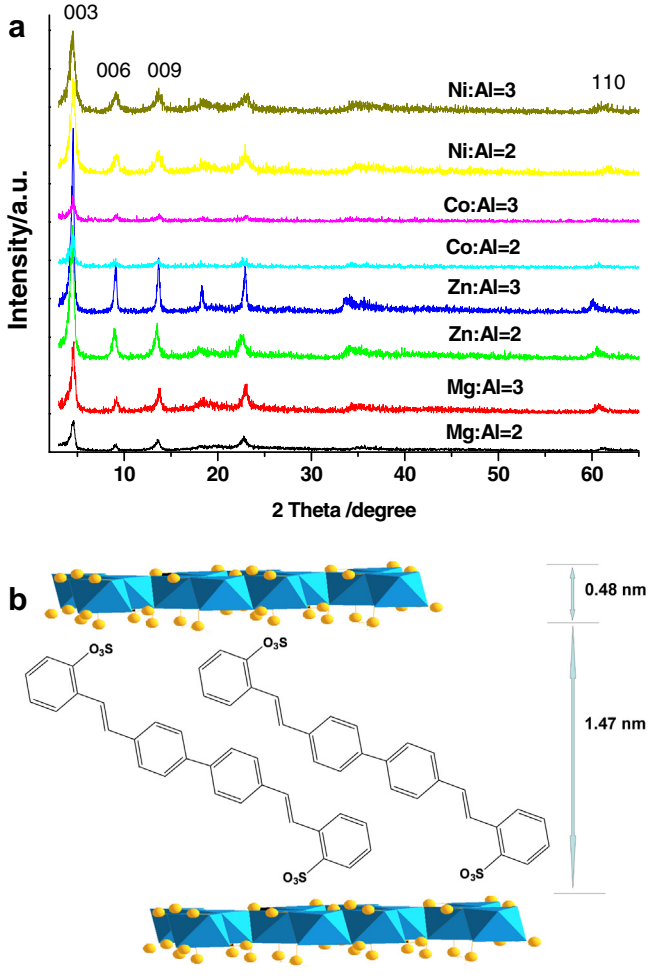

Fig. 1. (a) The XRD pattern of BSB/LDH powder samples and (b) structure model for BSB/Mg_2Al–LDH.

Table 1
Chemical compositions of BSB/LDHs.

Theoretical formula	Final M^{2+}/M^{3+}	Final chemical composition
$Mg_{0.666}Al_{0.333}(OH)_2(C_{28}H_{18}O_6S_2)_{0.165}nH_2O$	2.17	$Mg_{0.685}Al_{0.315}(OH)_2(C_{28}H_{18}O_6S_2)_{0.158}$ $0.56H_2O$
$Mg_{0.75}Al_{0.25}(OH)_2(C_{28}H_{18}O_6S_2)_{0.125}nH_2O$	2.96	$Mg_{0.747}Al_{0.253}(OH)_2(C_{28}H_{18}O_6S_2)_{0.127}$ $0.78H_2O$
$Zn_{0.666}Al_{0.333}(OH)_2(C_{28}H_{18}O_6S_2)_{0.165}nH_2O$	1.92	$Zn_{0.658}Al_{0.342}(OH)_2(C_{28}H_{18}O_6S_2)_{0.171}$ $1.13H_2O$
$Zn_{0.75}Al_{0.25}(OH)_2(C_{28}H_{18}O_6S_2)_{0.125}nH_2O$	2.99	$Zn_{0.749}Al_{0.251}(OH)_2(C_{28}H_{18}O_6S_2)_{0.125}$ $0.82H_2O$
$Co_{0.666}Al_{0.333}(OH)_2(C_{28}H_{18}O_6S_2)_{0.165}nH_2O$	2.00	$Co_{0.667}Al_{0.333}(OH)_2(C_{28}H_{18}O_6S_2)_{0.167}$ $0.71H_2O$
$Co_{0.75}Al_{0.25}(OH)_2(C_{28}H_{18}O_6S_2)_{0.125}nH_2O$	2.90	$Co_{0.744}Al_{0.256}(OH)_2(C_{28}H_{18}O_6S_2)_{0.128}$ $0.69H_2O$
$Ni_{0.666}Al_{0.333}(OH)_2(C_{28}H_{18}O_6S_2)_{0.165}nH_2O$	2.12	$Ni_{0.679}Al_{0.321}(OH)_2(C_{28}H_{18}O_6S_2)_{0.160}$ $0.96H_2O$
$Ni_{0.75}Al_{0.25}(OH)_2(C_{28}H_{18}O_6S_2)_{0.125}nH_2O$	2.59	$Ni_{0.721}Al_{0.279}(OH)_2(C_{28}H_{18}O_6S_2)_{0.140}$ $1.24H_2O$

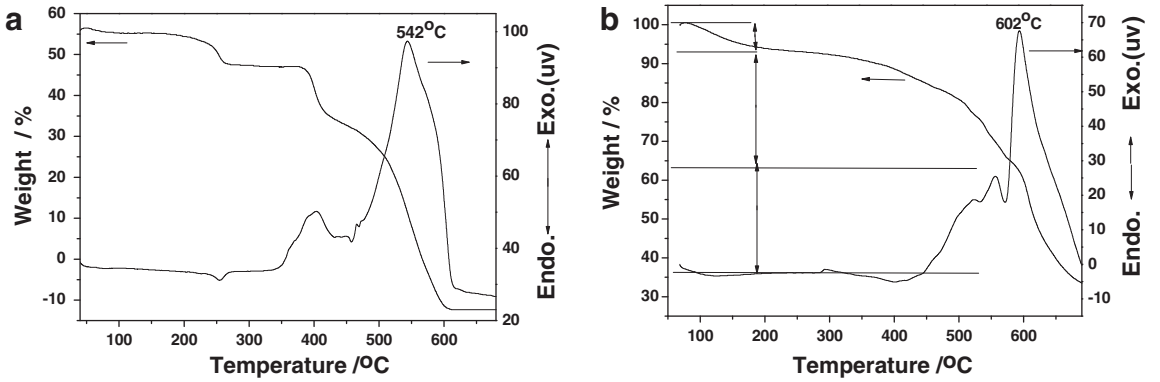

Fig. 2. Thermogravimetry and differential thermal analysis (TG–DTA) curves for (a) BSB, (b) BSB/Mg_2Al–LDH powder sample.

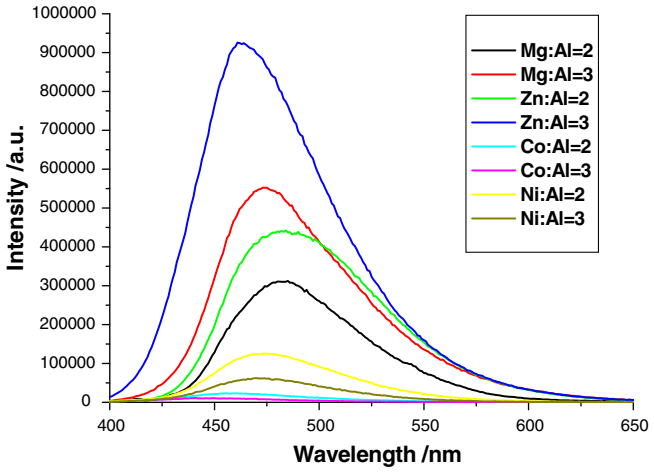

Fig. 3. Photoluminescent spectra of the BSB/LDH powder samples.

solution and solid UV–vis absorption spectra were collected in the range 220–800 nm on a Shimadzu U-3000 spectrophotometer, with the slit width of 1.0 nm and $BaSO_4$ as the reference. The solution and solid state fluorescence spectra were performed on RF-5301PC fluorospectrophotometer with the 360 nm excitation light. The width of both the excitation and emission slit is 3 nm. The fluorescence decays were measured using LifeSpec-ps spectrometer by 372 nm laser exciting for BSB and BSB/LDH samples, and the lifetimes were calculated with the F900 Edinburgh instruments software. Photoluminescence quantum yield (PLQY) and 1931 CIE color coordinates were measured using an HORIBA Jobin–Yvon FluoroMax-4 spectrofluorimeter, equipped with an F-3018 integrating sphere. Two-photon fluorescence of the samples was excited by 800 nm laser on a Tsunami–Spitfire-OPA-800C ultrafast optical parameter amplifier (Spectra Physics); two-photon absorption cross section for the pure BSB can be obtained by using the two-photon induced fluorescence measurement method with Rhodamine B as a reference. TG–DTA was measured on a PCT-1A thermal analysis system under ambient atmosphere with a heating rate of 10 °C/min. Elemental analysis was performed by ICP atomic emission spectroscopy on a Shimadzu ICPS-7500 instrument using the solutions prepared by dissolving the samples in dilute nitric acid. Carbon, hydrogen, nitrogen, and sulfur analyses were carried out using a Perkin–Elmer Elementarvario elemental analysis instrument.

3. Results and discussion

3.1. Structural characterization of BSB intercalated LDHs

Eight samples of BSB intercalated LDH composites, BSB/LDH (M^{II} = Mg^{2+}, Zn^{2+}, Co^{2+}, Ni^{2+}, and M^{III} = Al^{3+}) were prepared by the coprecipitation method. Their powder XRD patterns are shown in Fig. 1a. In each case, all the reflections can be indexed to a hexagonal lattice with *R-3m* rhombohedral symmetry, which is

Table 2
PLQY and CIE 1931 color coordinate of BSB/LDHs systems.

Sample	2:1 Zn:Al	3:1 Zn:Al	2:1 Co:Al	3:1 Co:Al	2:1 Ni:Al	3:1 Ni:Al	2:1 Mg:Al	3:1 Mg:Al	Pure BSB
PLQY(%)	21.9	45.2	1.2	0.5	3.5	0.7	17.8	27.0	19.0
Color coordinate	(0.166, 0.335)	(0.152, 0.182)	(0.217, 0.068)	(0.182, 0.119)	(0.122, 0.289)	(0.050, 0.388)	(0.154, 0.321)	(0.159, 0.260)	(0.145, 0.257)

commonly nominated as 3R-type LDH structure. Taking the BSB/MgAl–LDH (Mg:Al = 2) as an example, the main characteristic reflections appear at 4.49° (003), 9.07° (006), 13.54° (009) and 61.13° (110); the d_{003} (1.958 nm), d_{006} (0.974 nm) and d_{009} (0.653 nm) present a good multiple relationship for the basal, second and third-order reflections. The lattice parameter c can be calculated from averaging the positions of the three harmonics: $c = 1/3\ (d_{003} + 2d_{006} + 3d_{009})$. The basal spacing for BSB/Mg_2Al–LDH is 1.95 nm, which is consistent well with a single-layer arrangement model of the BSB anions in the LDH gallery (Fig. 1b). Considering the height of the LDH layer (0.48 nm), the spacing of the gallery between LDH layers is about 1.47 nm, which corresponds to the intercalated BSB anions being inclined at an angle of *ca.* 50° relative to the LDH layers. This arrangement fashion is close to that of the ultrathin film based on BSB and LDH nanosheets [19]. The lattice parameter a, which stands for the shortest distance of adjacent metal ions with identical chemical environment in the LDH layer, can be calculated by: $a = 2d_{110}$. For the BSB/MgAl–LDH (Mg:Al = 2) sample, the values of a is 0.304 nm, which is in accordance with other reported MgAl–LDH systems [13], further confirming its 3R-type LDH structure. Elemental analysis results (Table 1) show that the M^{2+}/M^{3+} molar ratios of the products are very close to the nominal ones, specially for the BSB/Mg_3Al–LDH, BSB/Zn_2Al–LDH, BSB/Zn_3Al–LDH, BSB/Co_2Al–LDH systems, suggesting the ordered LDH crystal structures for these samples.

Thermolysis behavior of BSB/LDH systems was further studied. Taking the BSB/Mg_2Al–LDH as an example (Fig. 2b), the thermal decomposition process can be characterized by three weight loss steps. The first one from room temperature to 190 °C is attributed to the removal of surface adsorbed and interlayer water molecules. The second one with a gradual weight loss (190–400 °C) involves both the decomposition of the BSB anions and the dehydroxylation of the brucite-like layers, accompanied by a board exothermic peak in the DTA curve. The third one corresponds to the collapse of the LDH layer and combustion of BSB with a strong exothermic peak at *ca.* 600 °C. Based on the comparison on the thermolysis process of BSB/LDH and pure BSB (Fig. 2a), it was concluded that the decomposition or combustion temperature of the BSB/LDH is higher than that of pure BSB by *ca.* 60 °C, indicating that the thermostability of BSB anions is enhanced upon intercalation within LDH.

3.2. Photophysical properties of BSB/LDHs

Fluorescent spectra of BSB/LDH samples were shown in Fig. 3. It can be observed that the emission intensity of BSB/Mg–Al–LDH and BSB/Zn–Al–LDH are systematically higher than those of BSB/Co–Al–LDH and BSB/Ni–Al–LDH samples, which can also be further concluded by comparing the photoluminescence quantum yield (PLQY) of the samples (Table 2). Such behaviors can be attributed to the emission is strongly reabsorbed by the Co- and Ni-containing LDH

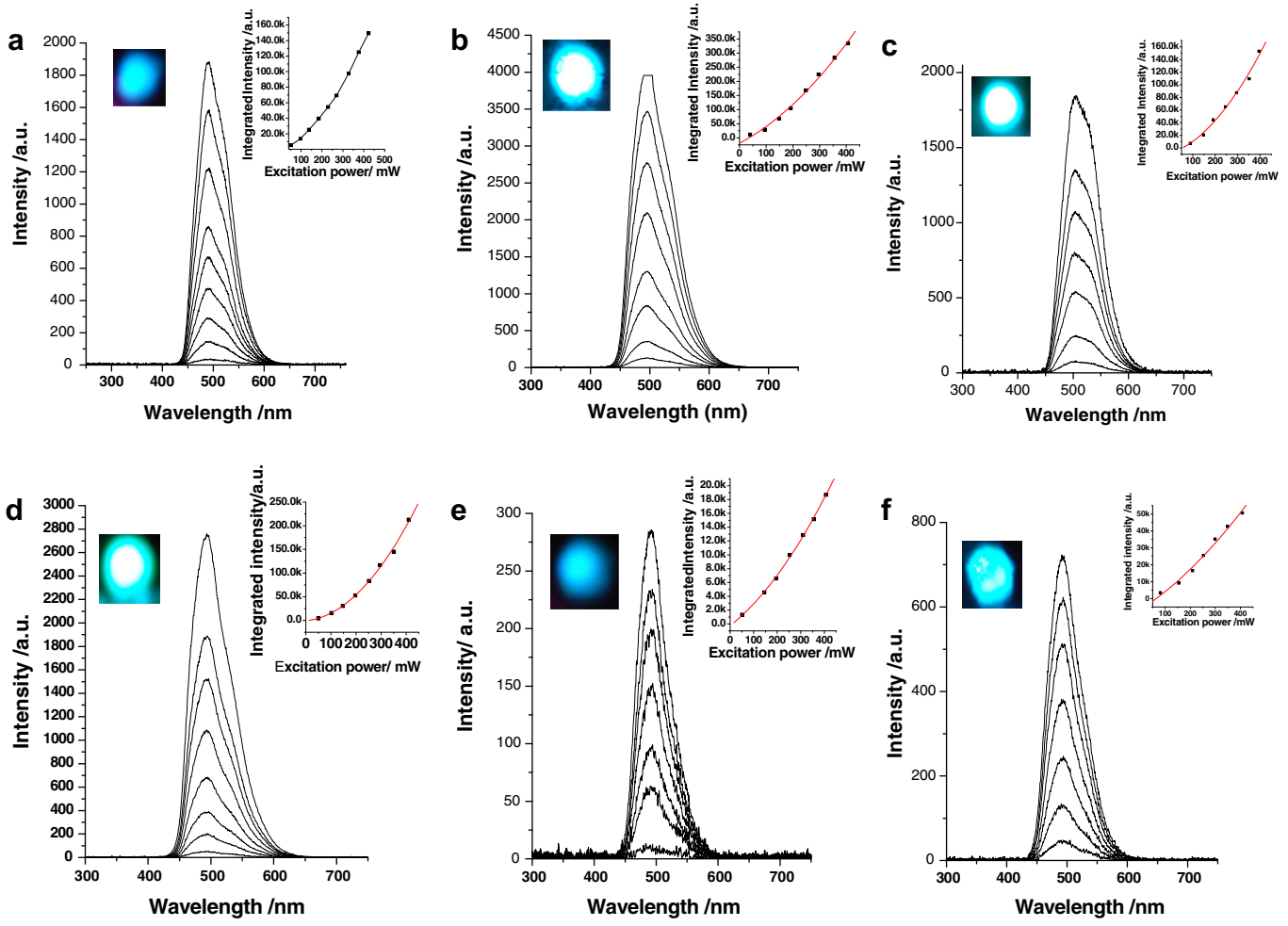

Fig. 4. Two-photon photoemission spectra of the BSB/LDH powder samples under 800 nm laser with increasing power (a) BSB/Mg_2Al–LDH, (b) BSB/Mg_3Al–LDH, (c) BSB/Zn_2Al–LDH, (d) BSB/Zn_3Al–LDH, (e) BSB/Ni_2Al–LDH,(f) BSB/Ni_3Al–LDH. Insets show the changes in integrated intensity at λ_{max}^{em} with increasing pump intensity.

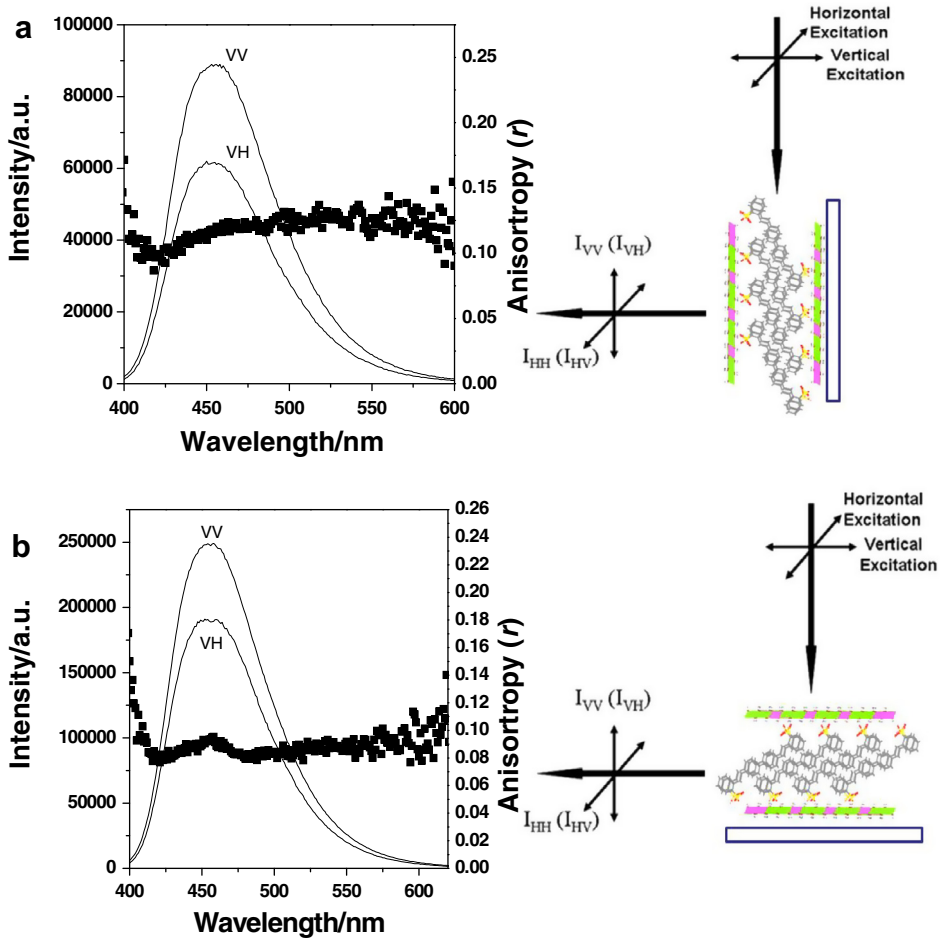

Fig. 5. One-photon polarized fluorescence profiles in the VV, VH modes and anisotropic value (r) for the BSB/LDH with the glancing (a) and vertical (b) incidence geometry of the excitation light (360 nm).

layers, which is confirmed by the UV–vis absorption spectra of the samples as shown in Fig. S1 in Supporting Information. As well, the heavy metals (such as Ni and Co) in the LDH layer can also result in the fluorescence quench. Moreover, PLQY values of three intercalation samples (BSB/Mg_3Al–LDH, BSB/Zn_2Al–LDH, BSB/Zn_3Al–LDH) are higher than the pristine BSB sample, suggesting the luminescent performance of the interlayer chromophore can be enhanced and tuned by choosing the suitable LDH layer. The highest PLQY value present at the BSB/Zn_3Al–LDH sample (45.2%), which is *ca.* 2.4-fold greater than the pristine BSB sample. Such improvement of the PLQY can be assigned to the better organization of the interlayer BSB unities with high crystalline degree in the gallery of LDH layer, which suppress the thermal vibration and rotation of stilbene anions effectively as demonstrated by XRD of BSB/Zn_3Al–LDH. In addition, compared with the pure BSB with the maximum emission wavelength (λ_{max}^{em}) located at 463 nm (Fig. S2 in Supporting Information), the BSB/LDH samples exhibit tunable λ_{max}^{em} in the range from 456 nm (BSB/Co_2Al–LDH) to 484 nm (BSB/Mg_2Al–LDH), demonstrating that the fluorescent wavelength can be continuously tuned by changing the layered charged density and chemical composition of LDH. The fluorescence lifetimes of both the BSB/Mg–Al–LDH and BSB/Zn–Al–LDH are close to the pure BSB powder sample (*ca.* 1.8 ns), and their fluorescent decay curves are shown in Fig. S3 in Supporting Information. In addition, based on the results of the CIE 1931 color coordinate (Table 2), it can be concluded that the emission of the intercalation products are mainly populated on the bluish green regions.

It was noted that the stilbene compound can be a two-photon absorption and emissive chromophore [2,18], and thus two-photon-excited fluorescence measurements were further made. The two-photon absorption cross section of pristine BSB is estimated as 1162 GM (1 GM = 10^{-5} cm^4 s $photon^{-1}$ $molecule^{-1}$) at 800 nm, which is comparable with that of other similar neutral stilbene-based compound [2]. In addition, for the BSB/Mg_2Al–LDH, a broad excitation band with the maximum peak at *ca.* 750 nm can be observed as shown in Fig. S4 in Supporting Information, suggesting that the samples can be solid-state two-photon fluorescence materials. Upon excitation by a 800 nm laser light, The BSB/ZnAl–LDH, BSB/MgAl–LDH, BSB/NiAl–LDH samples can exhibit strong fluorescence with the systematically red-shift emission of *ca.* 10–15 nm (Fig. 4) compared with those excited at 360 nm UV light. This phenomenon may be related to the fact that the high energy of laser can induce the reorganization and rearrangement of the BSB anion within the LDH layer, since the emission of BSB molecule is sensitive to the external stimuli [19]. Taking BSB/Mg_2Al–LDH as an example, the emissive spectra feature a narrow emission peak at 488 nm (Fig. 4a), and the emissive integrated intensity shows a nearly quadratic increase as a function of the excitation energy, further confirming the two-photon fluorescence from the samples. As a result, the as-prepared solid-state samples can also serve as organic–inorganic hybrid two-photon fluorescent materials with tunable emission wavelength. The two-photon emission that transfer from near-infrared (NIR) light to visible light can be easily visualized by the naked eye as shown inset of Fig. 4, suggesting

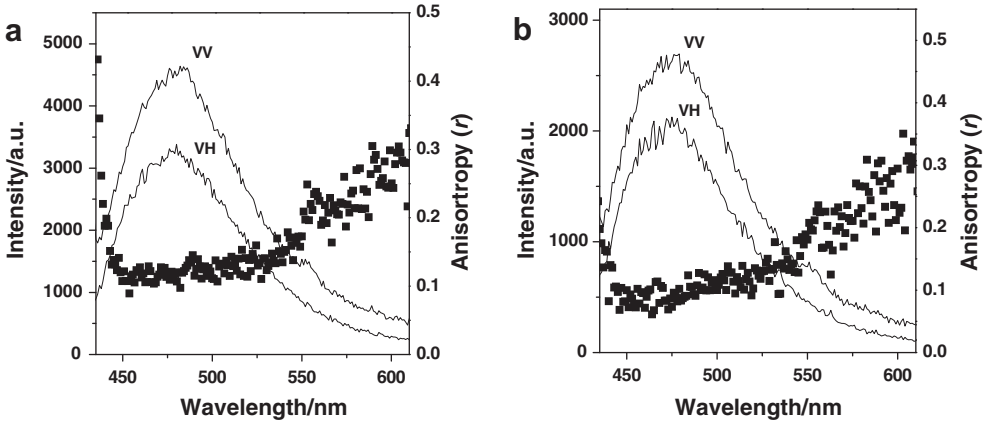

Fig. 6. Two-photon polarized emission fluorescence profiles in the VV, VH modes and anisotropic value (r) for the BSB/LDH with the glancing (a) and vertical (b) incidence geometry of the excitation light (800 nm).

that the BSB/LDH systems may be potentially served as NIR light detector. While for the BSB/CoAl–LDH, the two-photon fluorescence is relatively difficult to be detected due to the relative low PLQY value.

3.3. One-photon and two-photon polarized fluorescence of the BSB/LDH film

The BSB/Zn_3Al–LDH powder sample with highest PLQY was functionalized into thin film using a fabrication method of solvent evaporation. To further investigate the fluorescence polarization property and the microenvironment of BSB in the as-prepared BSB/LDH film, polarized fluorescence measurement was employed to probe the fluorescence anisotropic value r [20–22]. r can be expressed as the formula:

$$r = \frac{I_{VV} - GI_{VH}}{I_{VV} + 2GI_{VH}} \quad (1)$$

where $G = \frac{I_{HV}}{I_{HH}}$, determined from the BSB aqueous solution; I_{VH} stands for the PL intensity obtained with vertical polarized light excitation and horizontal polarization detection, and I_{VV}, I_{HH}, I_{HV} are defined in a similar way. Two typical measurement setups of polarized fluorescence (glancing and normal incidence geometry as shown in inset of Fig. 5) were employed to determine the fluorescence anisotropic value r. It was observed that, for the in-plane polarized excitation, the BSB/LDH film shows well-defined blue fluorescence anisotropy between the parallel and perpendicular to excitation polarized direction (I_{VV} vs. I_{VH}) with the anisotropic value (r) of *ca.* 0.12, which is slightly higher than the corresponding polarized excitation spectra in the range of 290–400 nm as shown in Fig. S5a in Supporting Information. In addition, the uniform r values in both the polarized excitation and emission spectra indicate that polarization scrambling via Förster transfer is minimal in the film, and also confirms the rigid-rod and isolated conformation of the BSB anions within the gallery. For the vertical polarized excitation (Fig. 5b), the I_{VV}/I_{VH} ratio is 1.30, lower than that of the horizontal excitation and vertical emission mode by *ca.* 10.7%. Moreover, based on the polarized fluorescence method [7], the orientational angle of the BSB molecule relative LDH layer can be estimated to be 30.4° (Fig. S6 in Supporting Information), which is consistent with the stacking fashions as indicated by the XRD.

Moreover, up-conversion polarized fluorescence was further detected by exciting the film at 800 nm. It can be shown that, in both the horizontal (Fig. 6a) and vertical (Fig. 6b) polarized excitation models, the film features well-defined up-conversion polarized photoemission. The fluorescence anisotropy in both the excitation (Fig. S5b in Supporting Information) and emission spectra are close to those excited at 360 nm, further confirming that fluorescent emission are derived from the process with one-photon and two-photon excited states to the ground state. To the best of our knowledge, BSB anions intercalated LDH system reported here may involve the first example of organic–inorganic hybrid material with the property of up-conversion polarized emission.

4. Conclusion

In summary, a sulfonated stilbene derivate (BSB) intercalated LDHs systems with different layer charge density and chemical composition have been prepared, and photoluminescent properties for both powder and film were investigated. The optimal fluorescent performance presents in the sample of BSB/Zn_3Al–LDH, in which the photoluminescence quantum yield of the BSB chromophore are largely enhanced upon intercalation, demonstrating that the immobilization of BSB anions between the rigid LDH galleries can suppress the nonradiative relaxation process effectively. Moreover, the BSB/LDH film was further fabricated, which present both one-photon and two-photon polarized photoemission. Therefore, the as-prepared film based on a stilbene anions regularly arranged within an inorganic LDH matrix may potentially serve as new types of up-conversion solid-state luminescence and polarized fluorescent materials.

Acknowledgments

This work was supported by the National Natural Science Foundation of China, the 111 Project (Grant No.: B07004), New Century Excellent Talents in University (NCET-11-0560) and Central University Research Funds.

Appendix A. Supplementary material

Supplementary data associated with this article can be found, in the online version, at http://dx.doi.org/10.1016/j.cej.2013.03.038.

Reference

[1] S.-J. Yoon, J.W. Chung, J. Gierschner, K.S. Kim, M.-G. Choi, D. Kim, S.Y. Park, Multistimuli two-color luminescence switching via different slip-stacking of highly fluorescent molecular sheets, J. Am. Chem. Soc. 132 (2010) 13675–13683.
[2] F. Gao, Q. Liao, Z. Xu, Y. Yue, Q. Wang, H. Zhang, H. Fu, Strong two-photon excited fluorescence and stimulated emission from an organic single crystal of an oligo(phenylene vinylene), Angew. Chem. Int. Ed. 49 (2010) 732–735.

[3] S.L. Oliveira, D.S. CorrTa, L. Misoguti, C.J.L. Constantino, R.F. Aroca, S.C. Zilio, C.R. Mendonça, Perylene derivatives with large two-photon-absorption cross-sections for application in optical limiting and upconversion lasing, Adv. Mater. 17 (2005) 1890–1893.
[4] S.R. Forrest, The path to ubiquitous and low-cost organic electronic appliances on plastic, Nature 428 (2004) 911–918.
[5] D.P. Yan, A. Delori, G.O. Lloyd, T. Friščić, G.M. Day, W. Jones, J. Lu, M. Wei, D.G. Evans, X. Duan, A cocrystal strategy to tune the luminescent properties of stilbene-type organic solid-state materials, Angew. Chem. Int. Ed. 50 (2011) 12483–12486.
[6] Z. Zhang, M.Y. Berezin, J.L.F. Kao, A. d' Avignon, M. Bai, S. Achilefu, Near-infrared dichromic fluorescent carbocyanine molecules, Angew. Chem. Int. Ed. 47 (2008) 3584–3587.
[7] F. López Arbeloa, V. Martínez. New fluorescent polarization method to evaluate the orientation of adsorbed molecules in uniaxial 2D layered materials, J. Photochem. Photobiol. A 181 (2006) 44–49.
[8] L.M. Maestro, J.E. Ramírez-Hernández, N. Bogdan, J.A. Capobianco, F. Vetrone, J. García Solé, D. Jaque, Deep tissue bio-imaging using two-photon excited CdTe fluorescent quantum dots working within the biological window, Nanoscale 4 (2012) 298–302.
[9] Z. Zhang, B. Xu, J. Su, L. Shen, Y. Xie, H. Tian, Color-tunable solid-state emission of 2,2′-biindenyl-based fluorophores, Angew. Chem. Int. Ed. 50 (2011) 11654–11657.
[10] M. Albota, D. Beljonne, J.L. Bredas, J.E. Ehrlich, J.Y. Fu, A.A. Heikal, S.E. Hess, T. Kogej, M.D. Levin, S.R. Marder, D. McCord-Maughon, J.W. Perry, H. Rockel, M. Rumi, C. Subramaniam, W.W. Webb, X.L. Wu, C. Xu, Design of organic molecules with large two-photon absorption cross sections, Science 281 (1998) 1653–1656.
[11] M. Ogawa, K. Kuroda, Photofunctions of intercalation compounds. Chemical, Review 95 (1995) 399–438.
[12] T.J. Vulica, A.F.K. Reitzmannb, K. Lázár, Thermally activated iron containing layered double hydroxides as potential catalyst for N_2O abatement, Chem. Eng. J. 166 (2011) 81–87.
[13] D.P. Yan, J. Lu, J. Ma, S. Qin, M. Wei, D.G. Evans, X. Duan, Layered host–guest materials with reversible piezochromic luminescence, Angew. Chem. Int. Ed. 50 (2011) 7037–7040.
[14] D.P. Yan, J. Lu, M. Wei, J. Han, J. Ma, F. Li, D.G. Evans, X. Duan, Ordered poly(*p*-phenylene)/layered double hydroxide ultrathin films with blue luminescence by layer-by-layer assembly, Angew. Chem. Int. Ed. 48 (2009) 3073–3076.
[15] J. Xu, S. Zhao, Z. Han, X. Wang, Y.F. Song, Layer-by-layer assembly of $Na_9[EuW_{10}O_{36}]\cdot 32H_2O$ and layered double hydroxides leading to ordered ultra-thin films: cooperative effect and orientation effect, Chem. Eur. J. 17 (2011) 10365–10371.
[16] C.H. Zhou, Z.F. Shen, L.H. Liu, S.M. Liu, Preparation and functionality of clay-containing films, J. Mater. Chem. 21 (2011) 15132–15153.
[17] H. Meier, Angew. Chem. Int. Ed. 44 (2005) 2482–2506.
[18] J.D. Wuest, Co-crystals give light a tune-up, Nat. Chem. 4 (2012) 74–75.
[19] D.P. Yan, J. Lu, M. Wei, J. Han, J. Ma, F. Li, D.G. Evans, X. Duan, Reversibly Thermochromic, Fluorescent Ultrathin Films with a Supramolecular Architecture, Angew. Chem. Int. Ed. 50 (2011) 720–723.
[20] D.P. Yan, J. Lu, M. Wei, D.G. Evans, X. Duan, Sulforhodamine B intercalated layered double hydroxide thin film with polarized photoluminescence, J. Phys. Chem. B 113 (2009) 1381–1388.
[21] P. Tang, Y. Feng, D. Li, Improved thermal and photostability of an anthraquinone dye by intercalation in a zinc–aluminium layered double hydroxide host, Dyes Pigm. 90 (2011) 253–258.
[22] B. Valeur, Molecular Fluorescence: Principles and Applications, Wiley-VCH, Verlag GmbH, 2001.